Color Correction with Lorentz boosts

Antoine Guennec, Nicoletta Prencipe, Edoardo Provenzi

Color Correction with Lorentz boosts

Antoine Guennec*[1], Nicoletta Prencipe†[1] and Edoardo Provenzi‡[1]

[1]Université de Bordeaux, CNRS, Bordeaux INP, IMB, UMR 5251, F-33400, 351 Cours de la Libération, Talence, France

Abstract

We show how to adapt the almost forgotten work of Yilmaz about the relativity of color perception to perform an automatic color correction of digital images through a three-dimensional version of Lorentz boosts used in the special theory of relativity. Even in this preliminary version, the resulting algorithm is robust and it outperforms the classical physically-based diagonal color correction techniques in terms of ability to remove color cast.

1 INTRODUCTION

Automatic color correction (ACC from now on) refers to the process of automatic removal of an unwanted color cast on a digital image generated by the presence of a non-neutral illuminant in the scene that is represented in the picture.

The Human Visual System (HVS from now on) is very good at naturally implementing an ACC thanks to the adaptation properties of both retinal cells and higher brain mechanisms. This explains why many ACC algorithms are based on the modeling of certain features of the HVS regarding color perception.

For a thorough exposition of ACC algorithms the interested reader can consult, e.g. [4] or [9]. Here, we will only recap the most important information that will allow us to remark the novelty of the algorithm that we will introduce in Section 3 with respect to the state of the art.

The nomenclature that will be used is the following: $\mathscr{I} \subset \mathbb{R}^2$ is the 2-dimensional support of a RGB digital image $\vec{I} = (I_R, I_G, I_B)$, where I_c is the RGB color channel of $\vec{I}$, $c \in \{R, G, B\}$. The position of the generic pixel belonging to $\mathscr{I}$ will be denoted by $x = (x_1, x_2)$ and the image intensity $I_c(x)$ is supposed to be normalized in $[0, 1]$.

The image formation model used in literature about ACC of single-illuminant digital images is the following:

$$I_c(x) = \rho_c(x) L_c, \qquad \forall c \in \{R, G, B\}, \tag{1}$$

where ρ_c is the c-component of the reflectance of the point in the scene represented by the pixel x and L_c is c-component of the illuminant present in the scene. It is very important to stress that, in spite of the appealing simplicity of this formula, eq. (1) is far from being an accurate description of the real image formation process. In fact, a more accurate formulation would be given by the so-called dichromatic model, see e.g. [4], which turns into eq. (1) under three very restrictive hypotheses:

1. there is no specular reflection in the scene;
2. the camera spectral sensitivity functions supports S_c are mutually disjoint;

*aguennecjacq@u-bordeaux.fr
†nicoletta.prencipe@math.u-bordeaux.fr
‡edoardo.provenzi@math.u-bordeaux.fr

3. the reflectance $\rho(x,\lambda)$ is constant for every $\lambda \in S_c$, in such a way that $\rho(x,\lambda)$ becomes separated into $\rho_R(x), \rho_G(x), \rho_B(x)$.

All ACC algorithms based on the image formation model represented by eq. (1) work in the same way: starting from the knowledge of $I_c(x)$ they want to estimate L_c in order to eliminate its presence, and so the unwanted color cast, by simple division. Of course, this inverse problem is ill-posed because in eq. (1) there is only one known quantity, i.e. $I_c(x)$, versus two unknown quantities, i.e. $\rho_c(x)$ and L_c.

To solve this ill-problem various solutions have been proposed in the literature, see again [4] or [9]. Here we just consider the two most widely used, which are based on the white-patch (WP) and the gray-world (GW) hypotheses. The first assumes that there is at least one patch with perfect reflectance in the visual scene, i.e. it exists $\bar{x}_c \in \Omega$ such that $\rho_c(\bar{x}_c) = 1$, so that $I_c(\bar{x}_c) = L_c$ for all $c \in \{R, G, B\}$ and $\rho_c^{WP}(x) = I_c(x)/I_c(\bar{x}_c)$ is a digital image without the color cast induced by the non-neutral illuminant.

The latter hypothesis assumes that the spatial average reflectance in a visual scene is achromatic. If we denote with $\bar{I}_c$ the spatial average of the image in the fixed chromatic channel c, then, it can be proved (see e.g. [9]) that, in this case, the digital image without color cast obtained assuming the GW hypothesis is given by $\rho_c^{GW}(x) = kI_c(x)/\bar{I}_c$, where $k \in (0,1)$ is the degree of achromatic value of the image, $k = 1/2$ being the middle gray.

We stress that real-world images do not satisfy these hypothesis all the time: a simple example is given by a close-up image, which will typically show uniform areas that violate the assumptions above.

Being represented by point-wise multiplications, the action of WP and GW ACC algorithms can be written in a diagonal form in this way:

$$\begin{pmatrix} I'_R(x) \\ I'_G(x) \\ I'_B(x) \end{pmatrix} = \begin{pmatrix} m_R & 0 & 0 \\ 0 & m_G & 0 \\ 0 & 0 & m_B \end{pmatrix} \begin{pmatrix} I_R(x) \\ I_G(x) \\ I_B(x) \end{pmatrix}, \tag{2}$$

where $m_c^{WP} = 1/I_c(\bar{x}_c)$ and $m_c^{GW} = k/\bar{I}_c$, for all $c \in \{R, G, B\}$.

2 YILMAZ'S MODEL OF COLOR PERCEPTION

In the paper [14], H. Yilmaz pioneered the mathematical treatment of color perception as a relative phenomenon. The analogies between special relativity theory and color perception that he proposed are innovative for both theoretical and applied purposes in the color context. Indeed, on one hand they are coherent with the intrinsic mathematical properties that a perceptual color space should have, see e.g. [10], [2], [11], [1] for further information; on the other hand, as we will see in section 3, under certain conditions, they will give us hints to develop a new ACC algorithm.

A full detailed version of the content of this section is available in the open access paper [8]. To fix the ideas let us start with the notation introduced by the author. It is a well known fact that the space of perceived colors is a convex cone of dimension 3, see again [11], or [13]. Yilmaz considers trichromatic observers who, after the adaptation to a certain broadband illuminant, can identify the colors they perceive through three coordinates: α, β, γ. Hence to each observer we associate a set of three orthonormal axes forming the basis $\mathscr{B} = \{\hat{\alpha}, \hat{\beta}, \hat{\gamma}\}$. The coordinates α and β are the so-called chromatic coordinates, which define the chromatic plane, while $\gamma > 0$ represents the *achromatic* coordinate, it goes from black to white through a gray scale. The γ-axis is also bounded from above by a certain $\gamma_{\max}$ because of glare. The chromatic plane can be re-parameterized using the polar coordinates ϕ, ρ instead of the cartesian ones α, β, through the formulas $\phi = \arctan(\beta/\alpha)$ and $\rho = \sqrt{\alpha^2 + \beta^2}$. ϕ and ρ represent the color's hue and chroma respectively. The set of variables ϕ, ρ, γ gives a cylindrical structure to the space. It is a customary choice to identify the directions of the axes $\hat{\alpha}$ and $\hat{\beta}$ with the opponent directions corresponding to the hues red-green and yellow-blue respectively, (this is the so-called Hering's opponency).

The saturation σ of a color is classically defined as the ratio between the chroma and its achromatic coordinate, $\sigma = \rho/\gamma$. The maximum perceivable saturation corresponds to spectral lights stimuli, Yilmaz denoted it with by the constant Σ. To summarize, the space of perceivable colors is restricted to the inner part of the truncated cone $\mathscr{C}$ depicted in Figure 1 and defined as follows:

$$\mathscr{C} = \{(\phi, \rho, \gamma) \in [0, 2\pi) \times \mathbb{R}_{>0} \times (0, \gamma_{\max}) | \rho < \Sigma\gamma\},$$

fully saturated spectral colors belong to the lateral surface of the cone $\partial\mathscr{C} = \{(\phi, \rho, \gamma) | \rho = \Sigma\gamma\}$.

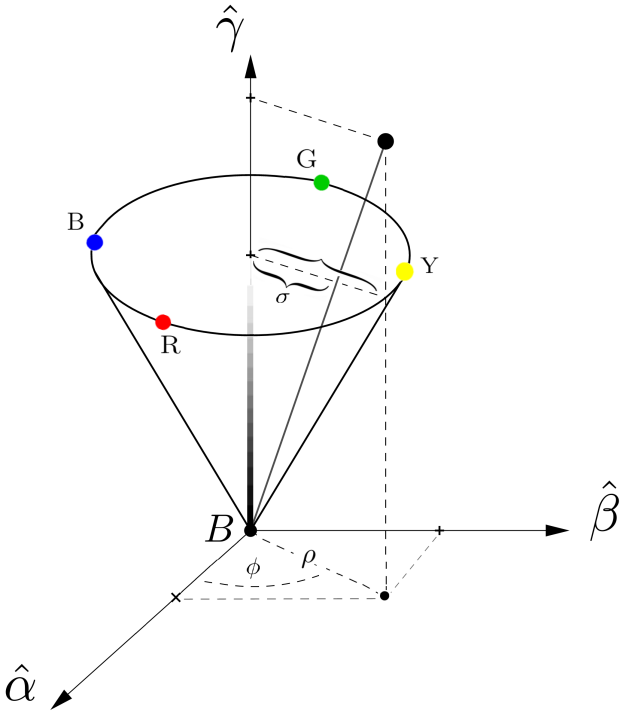

Figure 1: The cone of perceived colors $\mathscr{C}$.

Let us now consider two different broadband illuminants I and I'. An observer adapted to I (respectively I') describes the colors that he perceives with respect to the basis $\mathscr{B} = \{\hat{\alpha}, \hat{\beta}, \hat{\gamma}\}$ (respectively $\mathscr{B}' = \{\hat{\alpha}', \hat{\beta}', \hat{\gamma}'\}$), using the set of coordinates α, β, γ (or ϕ, ρ, γ) (respectively α', β', γ', or ϕ', ρ', γ'). In Yilmaz's work, the relationship between the two sets of variables (primed and unprimed) is claimed to be linear and represented by a matrix Ω. The explicit form for the nine entries $\{\Omega_{i,j}\}_{i,j=1,2,3}$ of Ω can be obtained as a result of three perceptual experiments. The experimental apparatus is composed by two identical rooms R_1 and R_2 illuminated by the light sources S_1 and S_2, respectively. R_1 and R_2 are separated by a common wall with a small hole which permits to an observer placed in R_i and adapted to S_i to look into the room R_j enlighten by S_j, $j \neq i$, i.e. an environment to which he/she is not adapted, $i, j = 1, 2$ and $i \neq j$. The walls are all painted in white and the observer is asked to judge the color of a piece of white paper divided into two parts, each one placed in one of the rooms, by matching it with a set of Munsell chips. In particular, he/she has to identify the perceived hue and saturation of the piece of white paper placed in his same room and the same for the other one perceived through the tiny hole. It is important to stress that in Yilmaz there is no context/background for the stimuli the observers are asked to identify: the object of his analysis is the change of color perception induced by an illuminant change before adaptation intervenes. Clearly the composition with a background transformation affects both the perceived hue and saturation, see [3, 11, 6]. Moreover, this model is made up for the perception of a single color stimulus, so its application developed in Section 3

to real-life complex images is clearly an approximation.

The constraints imposed to verify the results of a set of three experiments that Yilmaz claims to have performed with the experimental apparatus described above imply that the matrix Ω has the form of a Lorentz boost of amplitude σ along α-axis, the direction red-green, i.e. I' is seen to be reddish once observed by someone adapted to a greenish I. Mathematically:

$$\Omega_{\sigma,0} = \begin{pmatrix} \Gamma & 0 & -\sigma\Gamma \\ 0 & 1 & 0 \\ -\sigma\Gamma & 0 & \Gamma \end{pmatrix}, \qquad \Gamma = \frac{1}{\sqrt{1-\sigma^2}}, \tag{3}$$

the boost parameter σ is the perceived saturation of the piece of white paper, seen through the tiny hole. Of course, the red-green direction has nothing special: in order to obtain a boost matrix $\Omega_{\sigma,\phi}$ in the generic direction identified by the angle ϕ, it is sufficient to consider the ϕ-rotation matrix R_ϕ, i.e.

$$R_\phi = \begin{pmatrix} \cos\phi & -\sin\phi & 0 \\ \sin\phi & \cos\phi & 0 \\ 0 & 0 & 1 \end{pmatrix}, \tag{4}$$

and write $\Omega_{\sigma,\phi} = R_\phi \Omega_{\sigma,0} R_\phi^t$, recall that $R_\phi^{-1} = R_\phi^t$ because R_ϕ is an orthogonal matrix. By direct computation we get:

$$\Omega_{\sigma,\phi} = \begin{pmatrix} \Gamma\cos^2\phi + \sin^2\phi & (\Gamma-1)\cos\phi\sin\phi & -\sigma\Gamma\cos\phi \\ (\Gamma-1)\cos\phi\sin\phi & \Gamma\sin^2\phi + \cos^2\phi & -\sigma\Gamma\sin\phi \\ -\sigma\Gamma\cos\phi & -\sigma\Gamma\sin\phi & \Gamma \end{pmatrix}. \tag{5}$$

3 YILMAZ ACC: A NOVEL NON-DIAGONAL ALGORITHM FOR AUTOMATIC COLOR CORRECTION

As we have discussed in the previous section, Yilmaz's transformation allows us to pass from the coordinates of a color described by an observer adapted to a broadband illuminant I to those of an observer adapted to different broadband illuminant I'. In other terms, Yilmaz's transformation Ω is the matrix related to the change of basis of the same scene associated to two different illuminants.

The use of Yilmaz's model to perform ACC [1] is based on the following assumptions:

- the color perception of a scene by an observer adapted to its illuminant is identified by a digital image of the same scene taken under a neutral illuminant;
- instead, a digital image with color cast due to the presence of a non-neutral illuminant is identified with the color perception of an observer adapted to a neutral illuminant.

Following the assumptions above, it is natural, within the setting of Yilmaz's model, to perform an ACC of a digital image by applying the matrix Ω on it. This, of course, must be performed in the correct mathematical framework, as we are going to discuss.

We must transform the original RGB image into a cylindrical color space. The most adequate choice among this kind of color spaces available in the literature is given by the HCV (Hue Chroma Value) space. Indeed H corresponds to what we have called ϕ in the previous section, while C and V correspond to ρ and γ, respectively.

[1] We stress that the ACC performed via the Yilmaz transformation is relative only to the color correction part and *not* to the illuminant estimation, that is either performed manually, or given by the output of an illuminant estimation algorithm.

The conversion $(R,G,B)^t \mapsto (H,C,V)^t$ with $R,G,B \in [0,1]^3$ and $H \in [0,2\pi)$, $C,V \in [0,1]^2$ is implemented via these formulae:

$$\begin{cases} C := \max(R,G,B) - \min(R,G,B) \\ V := \max(R,G,B) \\ H := \frac{\pi}{3} \begin{cases} 0 & \text{if } C = 0 \\ \frac{G-B}{C} & \text{if } V = R \\ \frac{B-R}{C} + 2 & \text{if } V = G \\ \frac{R-G}{C} + 4 & \text{if } V = B \end{cases} \end{cases} . \tag{6}$$

In order to apply Yilmaz's transformation we need to have Cartesian coordinates in the chromatic plane, we denote them with α and β, respectively, keeping the value V unchanged, explicitly:

$$\begin{cases} \alpha = C\cos H \\ \beta = C\sin H \\ V = V \end{cases} . \tag{7}$$

By using primed letters to denote the coordinates of the image after Yilmaz's transformation, the ACC implemented by our algorithm can be written as follows:

$$\begin{pmatrix} \alpha \\ \beta \\ V \end{pmatrix} \longmapsto \begin{pmatrix} \alpha' \\ \beta' \\ V' \end{pmatrix} := \Omega_{\sigma,\phi} \begin{pmatrix} \alpha \\ \beta \\ V \end{pmatrix}, \tag{8}$$

where we apply to every pixel expressed in the coordinates $\alpha\beta V$, the matrix of a Lorentz boost $\Omega_{\sigma,\phi}$, whose explicit formulation is given by (5).

Note that if $\sigma = 0$, then $\Gamma = 1$ and $\Omega_{0,\phi}$ becomes the identity 3×3 matrix for all $\phi \in [0,2\pi)$, thus it does not produce any effect on the image.

The matrix $\Omega_{\sigma,\phi}$ depends on the two parameters σ and ϕ, that, in Yilmaz's model are, respectively, the saturation and the hue of a piece of white paper illuminated by the illuminant under which the observer is *not* adapted. We extrapolate these parameters from the picture thanks to the presence[2] of a color checker: we denote with W the RGB vector corresponding to a pixel of position $w \in \mathscr{I}$ belonging to the white square of the color checker. Hence $W = (R(w), G(w), B(w))^t \equiv (R_W, G_W, B_W)^t$. The parameters σ and ϕ correspond to the saturation and the hue of W, respectively, i.e. $\sigma = S(w)$ and $\phi = H(w)$, explicitly:

$$\sigma = \frac{C(w)}{V(w)} = \frac{\max(R_W,G_W,B_W) - \min(R_W,G_W,B_W)}{\max(R_W,G_W,B_W)}, \tag{9}$$

$$\phi = \frac{\pi}{3} \begin{cases} 0 & \text{(a)} \\ \frac{G_W - B_W}{\max(R_W,G_W,B_W)} \mod 6 & \text{(b)} \\ \frac{B_W - R_W}{\max(R_W,G_W,B_W)} + 2 & \text{(c)} \\ \frac{R_W - G_W}{\max(R_W,G_W,B_W)} + 4 & \text{(d)} \end{cases} \tag{10}$$

where (a) is $\max(R_W,G_W,B_W) = 0$, (b) is $\max(R_W,G_W,B_W) = R_W$, (c) is $\max(R_W,G_W,B_W) = G_W$ and (d) is $\max(R_W,G_W,B_W) = B_W$.

We apply the matrix $\Omega_{\sigma,\phi}$ to each pixel as indicated in eq. (8) obtaining:

$$\begin{cases} \alpha' = (\Gamma\cos^2\phi + \sin^2\phi)\,\alpha + (\Gamma - 1)\cos\phi\sin\phi\,\beta - \sigma\Gamma\cos\phi\,V \\ \beta' = (\Gamma - 1)\cos\phi\sin\phi\,\alpha + (\Gamma\sin^2\phi + \cos^2\phi)\,\beta - \sigma\Gamma\sin\phi\,V \\ V' = -\sigma\Gamma\cos\phi\,\alpha - \sigma\Gamma\sin\phi\,\beta + \Gamma\,V. \end{cases} \tag{11}$$

[2]For pictures without color checker we have chosen manually a pixel $w \in \mathscr{I}$ supposed to be white.

In order to show the transformed picture on a monitor, we need to come back to the RGB representation. For this, we pass from Cartesian to polar coordinates, leaving the value V' unchanged, as follows:

$$\begin{cases} H' = \arctan(\beta'/\alpha') \\ C' = \sqrt{\alpha'^2 + \beta'^2} \\ V' = V' \end{cases} . \tag{12}$$

Finally, by using the classical colorimetric formulae to pass from the HCV space to RGB, we obtain the transformed values (R', G', B').

4 Results

We have tested the Lorentz ACC algorithm on several pictures of natural scenes. The first two, shown in Figure 2, belong to the open access ColorChecker dataset available at the following website: https://colorconstancy.com/evaluation/datasets/, a dataset that was created with the purpose of testing illuminant estimation algorithms. The specificity of this dataset is that no color cast correction was performed and a color checker is present on each image.

We used it to test our correction algorithm, taking as ground truth vector the RGB coordinates of a pixel belonging to the white square of the color checker. We defined a Lorentz boost matrix $\Omega_{\sigma,\phi}$ as in Formula 5 setting the parameters σ and ϕ appearing in the matrix to be the saturation and hue of the ground truth vector, and applying it pixelwise. We must stress that our method only needs to extract two parameters from the three dimensional vector associated to the illuminant: the hue and the saturation. This means that different ground truth vectors with e.g. the same hue and saturation, but different value would lead to the same correction matrix. On a final note, the images presented here in Figure 2 and 3 that compare our algorithm with the usual diagonal correction implied by using eq. (2) were processed by using a white patch illuminant estimation and were selected such that we avoid any clipping.

4.1 Visual Comparison of the Results

A visual analysis of the pictures shown in the previous figures shows that the Yilmaz transformation algorithm shows pros and cons with respect to the diagonal correction. By considering the residual yellowish and organish color cast left by the diagonal algorithm on the left hand side of the third line of Figure 2 and on the cat image, respectively, it seems that Yilmaz transform is able to better eliminate the color cast.

On the contrary, by looking at the color checker, it can be seen that the Yilmaz transform still needs to be finely tuned with respect to the hue rendering. See also Section 6 for more insights about this issue.

Another intriguing feature of the Yilmaz ACC method w.r.t. the diagonal one is that, as it can be seen from the results, the first preserves the intensity sensation (called brightness from now on), whereas the latter does not; this effect is particularly noticeable in pictures on the left hand column of Figure 3. In order to explain this effect, we have to search for a quantity that is left invariant by the Lorentz boost operated by the Yilmaz transform. The most natural Lorentz-invariant quantity is the Minkowski norm [7] of a pixel $x \in \Omega$ in the HCV space, which is defined as follows:

$$\mathcal{M}(x) = \sqrt{V(x)^2 - C(x)^2}, \quad \forall x \in \Omega. \tag{13}$$

Therefore, we are led to conjecture that the brightness of a pixel x can be identified with its Minkowski norm $\mathcal{M}(x)$.

To reinforce our conjecture, we observe that, if we use the Minkowski norm to display the gray levels of the pixels in a digital image, we get a perfectly coherent picture with the usual gray level representation, as it is shown in Figure 4.

Notice that the aim of the Yilmaz ACC is not, at least in this paper, an image enhancement, but a perceptually coherent color correction. However, for the sake of a comparison with similar

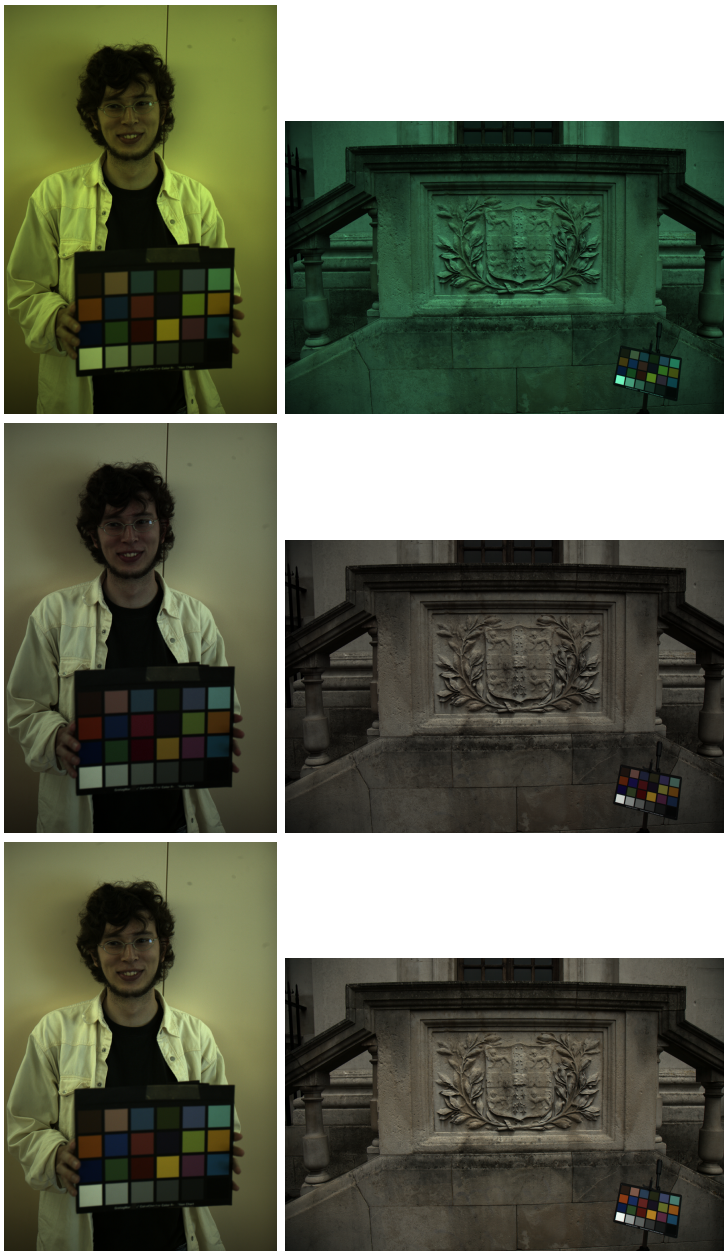

Figure 2: Top: original images from ColorChecker dataset. Middle: result of Yilmaz's ACC algorithm. Bottom: diagonal correction.

intensities, we show the 'books image' with a simple gamma correction alongside the result of the diagonal algorithm in Figure 5.

Furthermore, we also ran experiments to test the robustness of our algorithm w.r.t. (broad-band) illuminant changes of a fixed scene. For this, we used the dataset YACCD, see [12]. Our results, depicted in Figure 6, show that the output images of the Yilmaz algorithm are almost perceptually indistinguishable. Notice that the YACCD pictures are purposely affected by random noise in order to challenge an automatic illuminant estimation. For this reason, we have selected the illuminant parameters by using a pixel in the white '@ sign' on the cube. As it can be seen in 6, while our method is free from artifacts, the diagonal ones are not.

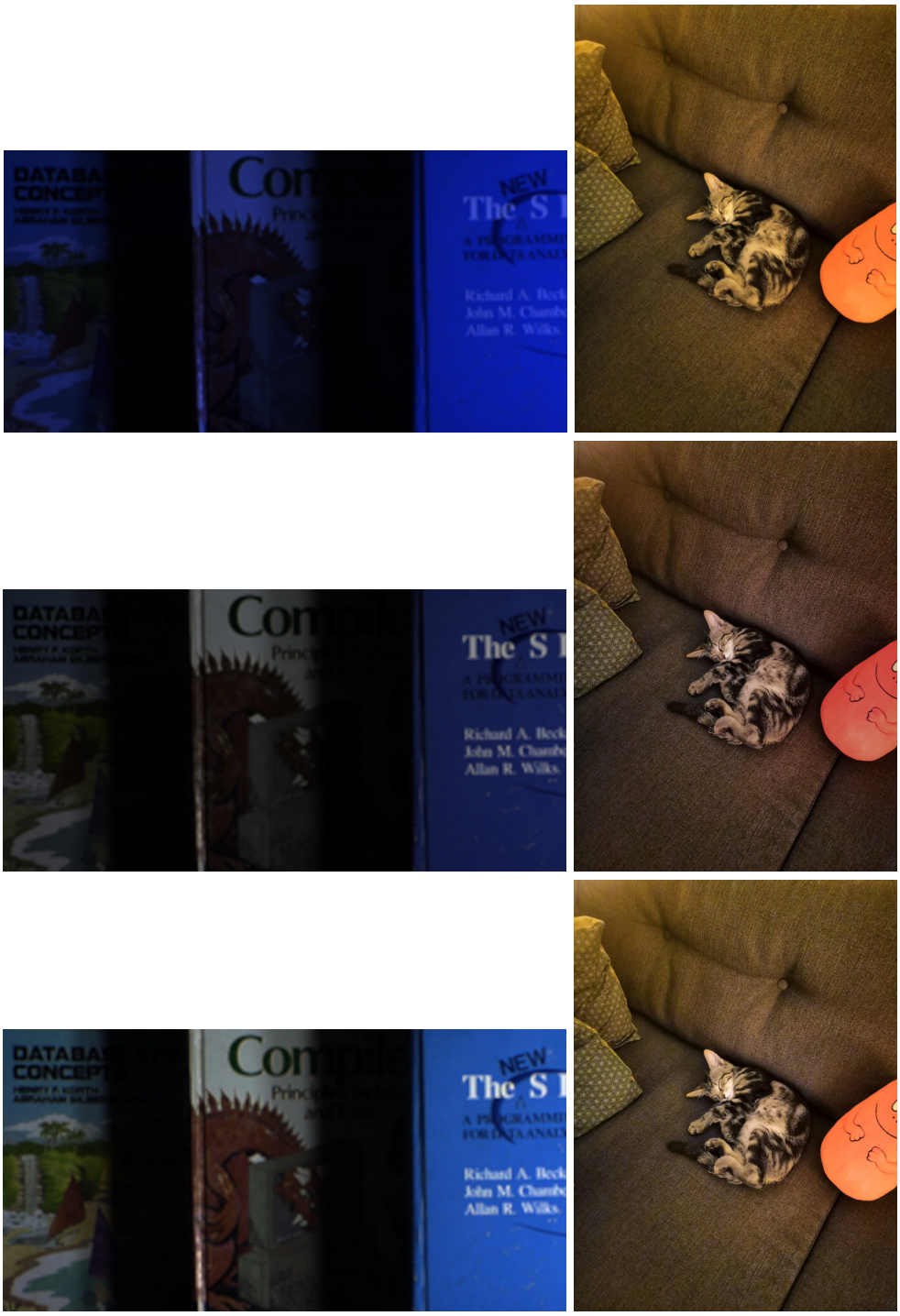

Figure 3: Top: original images. Middle: result of Yilmaz's ACC algorithm. Bottom: diagonal correction.

5 Analysis of Artifacts

One common problem of ACC algorithms is that, depending on the illuminant estimation, clipping can occur (notably in multi-illuminant scenes). This supplementary clipping process leads to false

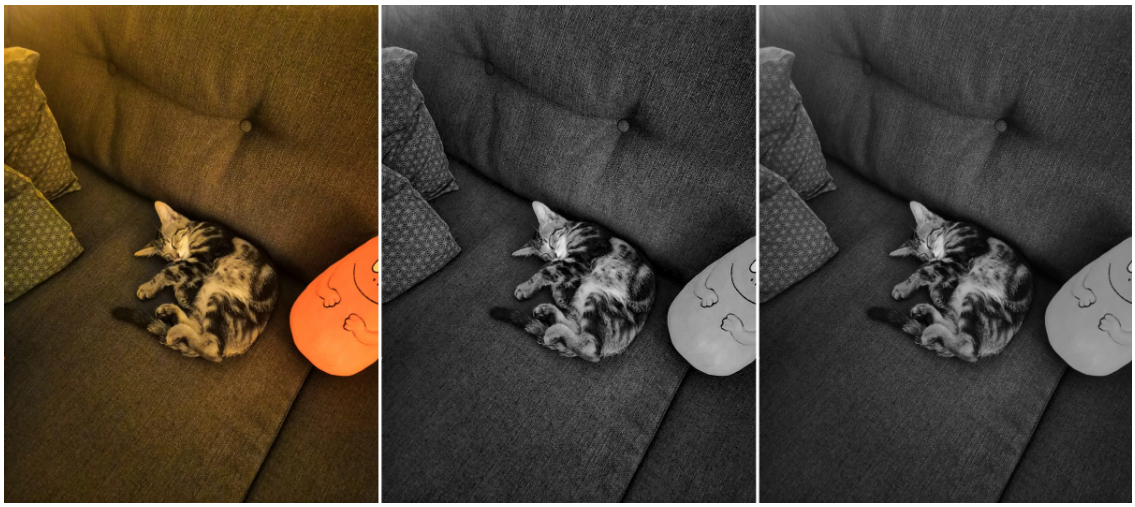

Figure 4: Left: original image. Middle: gray level version obtained by exhibiting the Minkowski norm of each pixel. Right: gray level version computed via the formula $(R(x) + G(x) + B(x))/3$ for all $x \in \Omega$.

Figure 5: Left: Yilmaz correction with an additional gamma correction of $\gamma = 0.7$. Right: diagonal correction as in Figure 3.

colors and artefacts. Unfortunately this is also the case for the Yilmaz method, as we have shown in Figure 7 (observe the curtain and the white patch on the color checker present in the image).

In order to mathematically analyze these artifacts we follow the transformations of a white pixel y, i.e. $(R(y), G(y), B(y))^t = (1, 1, 1)^t$ after the application of our algorithm:

$$\begin{pmatrix} 1 \\ 1 \\ 1 \end{pmatrix} \mapsto \begin{pmatrix} -\sigma\Gamma\cos\phi \\ -\sigma\Gamma\sin\phi \\ \Gamma \end{pmatrix} \mapsto \begin{pmatrix} \phi + \pi \\ \sigma\Gamma \\ \Gamma \end{pmatrix} \mapsto \begin{pmatrix} \Gamma(1-\sigma) \\ \Gamma \\ \Gamma(1-\sigma) \end{pmatrix}. \tag{14}$$

We list next the interpretation of the artifacts that we can infer from the computation above.

1. $V'(y) = \Gamma = \frac{1}{\sqrt{1-\sigma^2}} \geq 1$ and $\Gamma = 1 \iff \sigma = 0$. However, as already remarked, if $\sigma = 0$ no correction is performed. Thus, whenever $\sigma \neq 0$, there will be an artefact at the pixel of position y on the output image.
2. $H'(y) = \phi + \pi$, which explains why the hue of the artefact is opposite w.r.t. that of the illuminant.

From a theoretical point of view, Lorentz boosts preserve the inner part of the cone, so it is impossible to have points falling outside the cone through its lateral surface (because of the intrinsic nature of the transformation). However, while in special relativity the future light cone is

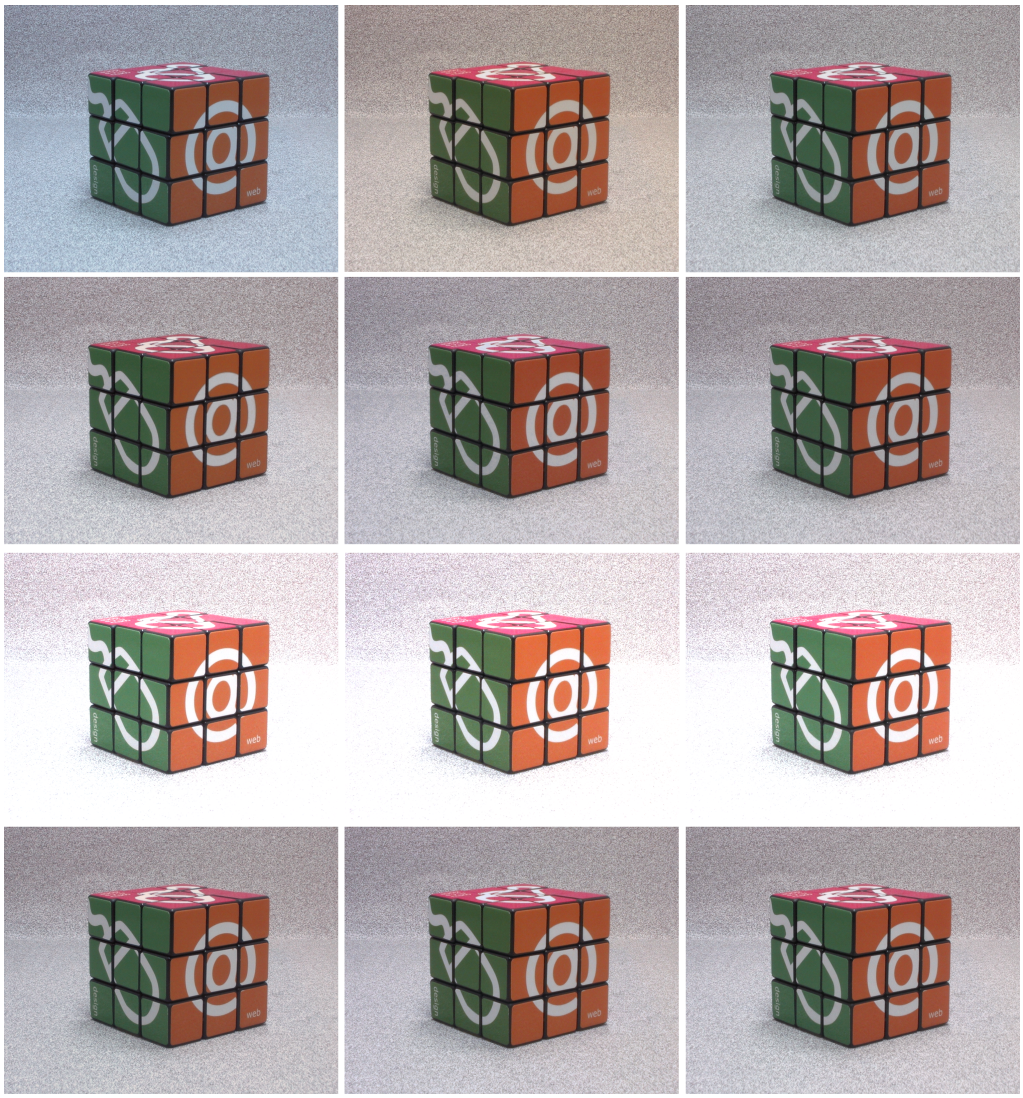

Figure 6: First row: images of the same scene taken under three different illuminants. Second row: Yilmaz correction of the image above. Third row: outputs of the diagonal method with artifacts. Forth row: diagonal method with clipping to remove the artifacts.

Figure 7: Left: original image. Middle: Yilmaz correction. Right: diagonal correction. The illuminant estimation in both corrections was done using the white square present on the color checker.

infinite, the HCV cone is truncated at $V = 1$, hence there are points falling outside the truncation

level after performing a Lorentz boost.

Let us write explicitly the condition $V' > 1$ that identifies the transformed pixels which have fallen outside the HCV cone as a function of the original HCV values. To this aim, let us rewrite the third equation in (11) in terms of H and C, i.e.:

$$V' = \Gamma(V - \sigma\, C \cos(\phi - H)) \tag{15}$$

and impose $V' > 1$:

$$V' = -\sigma\Gamma \cos\phi\, C \cos H - \sigma\Gamma \sin\phi\, C \sin H + \Gamma\, V > 1, \tag{16}$$

by using the cosine addition formula we obtain $-\sigma\Gamma C \cos(\phi - H) + \Gamma V > 1$, i.e.

$$\sigma C \cos(\phi - H) < V - \frac{1}{\Gamma},$$

so that:

$$V' > 1 \iff \sigma C \cos(\phi - H) < V - \sqrt{1 - \sigma^2}. \tag{17}$$

Our tests have shown that the pixels presenting artefacts in the output image are precisely those satisfying the condition (17). To correct these artifacts, we can either choose not to filter the pixels verifying this condition, or we can detect them and:

1. clip their value of those so that $V' = 1$;
2. add an angle π to H', thus avoiding the hue shift.

Figure 8 shows the result of this artifact-prevention technique on the image shown in Figure 7.

Figure 8: Left: original image. Right: Yilmaz correction. The pixels that were supposed to be clipped after the correction have been left unchanged from the original image.

As it can be seen, this technique does not eliminate all the artifacts: some low-saturated pixels can have their saturation augmented and their hue transformed as follows $\simeq \phi + \pi$, where ϕ is the estimated illuminant's hue. The investigation about how to automatically correct these artifacts is still ongoing.

6 CONCLUSIONS AND FUTURE PERSPECTIVES

We have introduced and discussed, both theoretically and experimentally, a novel ACC method inspired by the almost forgotten ideas of Yilmaz [14], who argued that a 3D version of Lorentz transformations describes the change of color coordinates between observers adapted to different broadband illuminants. We have explained how to adapt Yilmaz's ideas to image processing

obtaining an computationally efficient algorithm able to perform ACC once the illuminant estimation is known. Even if we consider it a preliminary version of a more complete algorithm, its performances are surprisingly good and, as we have shown, usually even better than the classical physically-based diagonal methods for ACC.

Differently from these techniques, our algorithm does not run in the RGB space, but in a cylindrical one. Actually, we consider that the approximations and clippings embedded in the classical colorimetric equations to pass from RGB to cylindrical color spaces may be responsible for some of the artifacts that we have experienced, e.g. the effect of the Yilmaz transform on the color checker patches stressed in Section 4. For this reason, a future investigation that we are going to perform is the possibility to define a more suitable way to implement this color space transformation.

Finally, a further examination of the achromatic coordinate coherent with Weber-Fechner's law [5] is of crucial importance to obtain a completely coherent perceptual ACC algorithm.

ACKNOWLEDGEMENTS

The authors wish to thank Ghalia Hemrit and Joseph Meenhan for useful discussions about the application of Yilmaz's paper to ACC. We also acknowledge the support by Huawei Technologies France SASU.

References

[1] A. Ashtekar, A. Corichi, and M. Pierri. Geometry in color perception. *Black Holes, Gravitational Radiation and the Universe*, pages 535–550, 1999.

[2] M. Berthier. Geometry of color perception. Part 2: perceived colors from real quantum states and Hering's rebit. *The Journal of Mathematical Neuroscience*, 10(1):1–25, 2020.

[3] M.D. Fairchild. *Color appearance models*. Wiley, 2005.

[4] Arjan Gijsenij, Theo Gevers, and Joost Van De Weijer. Computational color constancy: Survey and experiments. *IEEE Transactions on Image Processing*, 20(9):2475–2489, 2011.

[5] B.E. Goldstein. *Sensation and Perception, 9th Edition*. Cengage Learning, 2013.

[6] G. Gronchi and E. Provenzi. A variational model for context-driven effects in perception and cognition. *Journal of Mathematical Psychology*, 77:124–141, 2017.

[7] Barrett O'Neill. *Semi-Riemannian geometry with applications to relativity*. Academic press, 1983.

[8] N. Prencipe, V. Garcin, and E. Provenzi. Origins of hyperbolicity in color perception. *J. Imaging*, 6:42, June 2020.

[9] Edoardo Provenzi. *Computational Color Science: Variational Retinex-like Methods*. John Wiley & Sons, 2017.

[10] Edoardo Provenzi. Geometry of color perception. part 1: structures and metrics of a homogeneous color space. *The Journal of Mathematical Neuroscience*, 10(1):1–19, 2020.

[11] H.L. Resnikoff. Differential geometry and color perception. *Journal of Mathematical Biology*, 1:97–131, 1974.

[12] A. Rizzi, C. Gatta, and D. Marini. Yaccd: Yet another color constancy database. In *Proc. of El. Im. 2003, IS&T/SPIEs International Symposium, Color Imaging VIII San Jose, California (USA)*, volume 5008, pages 24–35, 2003.

[13] E. Schrödinger. Grundlinien einer theorie der farbenmetrik im tagessehen (Outline of a theory of colour measurement for daylight vision). Available in English in Sources of Colour Science, Ed. David L. Macadam, The MIT Press (1970), 134-82. *Annalen der Physik*, 63(4):397–456; 481–520, 1920.

[14] H. Yilmaz. Color vision and a new approach to general perception. *Biological Prototypes and Synthetic Systems*, pages 126–141, 1962.